Neuroscience 162 (2009) 959–971

TUMOR NECROSIS FACTOR ALPHA AND INTERFERON GAMMA COOPERATIVELY INDUCE OXIDATIVE STRESS AND MOTONEURON DEATH IN RAT SPINAL CORD EMBRYONIC EXPLANTS

M. MIR,[a] V. J. ASENSIO,[a] L. TOLOSA,[a] M. GOU-FABREGAS,[b] R. M. SOLER,[b] J. LLADÓ[a] AND G. OLMOS[a]*

[a]*Grup de Neurobiologia Cel.lular, Institut Universitari d'Investigacions en Ciències de la Salut (IUNICS)/Departament de Biologia, Universitat de les Illes Balears, Cra. de Valldemossa, km 7.5, E-07122 Palma de Mallorca, Illes Balears, Spain*

[b]*Unitat de Senyalització Neuronal, Departament de Ciències Mèdiques Bàsiques, Facultat de Medicina, Universitat de Lleida-IBRLLEIDA, Montserrat Roig, 2, E-25008-Lleida, Spain*

Abstract—The accumulation of reactive microglia in the degenerating areas of amyotrophic lateral sclerosis (ALS) tissue is a key cellular event creating a chronic inflammatory environment that results in motoneuron death. We have developed a new culture system that consists in rat spinal cord embryonic explants in which motoneurons migrate outside the explant, growing as a monolayer in the presence of glial cells. The proinflammatory cytokines tumor necrosis factor alpha (TNF-α) and interferon gamma (IFN-γ) have been proposed to be involved in ALS-linked microglial activation. In our explants, the combined exposure to these cytokines resulted in an increased expression of the pro-oxidative enzymes inducible nitric oxide synthase (iNOS), the catalytic subunit of the nicotinamide adenine dinucleotide phosphate (NADPH) oxidase, gp91^{phox} and cyclooxygenase-2 (COX-2), as compared to each cytokine alone. This effect was related to their cooperation in the activation of the transcription factor nuclear factor kappa B (NF-κB). TNF-α and IFN-γ also cooperated to promote protein oxidation and nitration, thus increasing the percentage of motoneurons immunoreactive for nitrotyrosine. Apoptotic motoneuron death, measured through annexin V-Cy3 and active caspase-3 immunoreactivities, was also found cooperatively induced by TNF-α and IFN-γ. Interestingly, these cytokines did not affect the viability of purified spinal cord motoneurons in the absence of glial cells. It is proposed that the proinflammatory cytokines TNF-α and IFN-γ have cooperative/complementary roles in inflammation-induced motoneuron death.

*Corresponding author. Tel: +34-971-17-24-48; fax: +34-971-17-31-84.
E-mail address: gabriel.olmos@uib.es (G. Olmos).

Abbreviations: ALS, amyotrophic lateral sclerosis; AMT, 4H-1,3-thiazin-2-amine, 5,6-dihydro-6-methyl-hydrochloride; ANOVA, analysis of variance; BSA, bovine serum albumin; COX-2, cyclooxygenase-2; DAB, diaminobenzidine; DNPH, 2,4-dinitrophenylhydrazine; GFAP, glial fibrillary acidic protein; IFN-γ, interferon gamma; iNOS, inducible nitric oxide synthase; LPS, lipopolysaccharide; MAP2, microtubule-associated protein 2; NADPH, nicotinamide adenine dinucleotide phosphate; NF-κB, nuclear factor kappa B; NHS, normal horse serum; NO, nitric oxide; PBS, phosphate-buffered saline; SDS, sodium dodecyl sulfate; SOD1, superoxide dismutase 1; TBS, Tris buffer saline; TNF-α, tumor necrosis factor alpha; VAChT, vesicular acetylcholine transporter.

Key words: amyotrophic lateral sclerosis, microglia, neuroinflammation, nitric oxide, proinflammatory cytokines.

Amyotrophic lateral sclerosis (ALS) is a progressive neurodegenerative disease characterized by degeneration of motor cortex, brain stem and spinal cord motoneurons (Shaw, 2005). ALS was traditionally regarded as a "neuron only disease," however, increasing evidences have demonstrated that glial cells, in particular activated microglia, may contribute to the initiation and progression of this disease (Sargsyan et al., 2005; Weydt and Moller, 2005; Boillee et al., 2006).

ALS tissue is characterized by neuroinflammatory changes observed in both sporadic and familial ALS and in the superoxide dismutase 1 (SOD1) transgenic mouse model of ALS (McGeer and McGeer, 2002; Mhatre et al., 2004; Weydt and Moller, 2005). The key cellular event signaling the presence of neuroinflammation in ALS is the accumulation of reactive microglia in the degenerating areas (Henkel et al., 2004; Turner et al., 2004; Sargsyan et al., 2005). The microglial reactivity is initiated before motoneuron loss (Hall et al., 1998; Henkel et al., 2006), suggesting that microglia are activated early in the pathogenesis of ALS, either sensing the earliest neuronal stress or triggering the process. In accordance with this microglial activation, numerous systemic immune alterations have been described both in ALS patients and in the transgenic mouse model (Zhang et al., 2005; Banerjee et al., 2008; Holmoy, 2008). Several studies have reported T cell (CD4, CD8 and CD40 positive) infiltration along the vessel walls of the spinal cord and brain of ALS patients (Troost et al., 1989; Kawamata et al., 1992; Graves et al., 2004); these activated T cells may directly activate macrophages/microglia through cell–cell contact or may release their own inflammatory mediators, in particular, the proinflammatory cytokine interferon gamma (IFN-γ), one of the most potent microglia-activating factors (Hanisch, 2002). IFN-γ-activated microglia are, in turn, a source of the proinflammatory cytokine tumor necrosis factor alpha (TNF-α) (Hanisch, 2002). This cytokine has been demonstrated to be an autocrine/paracrine signal for microglia and proposed to be implicated in the chronic activation of microglia observed in neurodegenerative disorders (Ghezzi and Mennini, 2001; Kuno et al., 2005). In this regard, increased levels of the cytokines IFN-γ and TNF-α have been reported in the blood of ALS patients (Poloni et al., 2000; Babu et al., 2008) and in the spinal cord of the transgenic mouse model (Elliott, 2001; Hensley et al., 2003).

0306-4522/09 $ - see front matter
doi:10.1016/j.neuroscience.2009.05.049

Among the secretion products of activated microglia, nitric oxide (NO), produced after the induction of type II nitric oxide synthase (iNOS) in microglia, plays a critical role in mediating neurotoxicity associated with the neuroinflammation process (Dawson and Dawson, 1998). We have recently addressed the interaction between IFN-γ and TNF-α in the regulation of NO generation in pure microglial cultures and have demonstrated that both cytokines are required, through a very specific interplay, for the up-regulation of the iNOS (Mir et al., 2008). In this study, we have developed a new culture system to assess the functionality of spinal cord motoneurons in the presence of microglia: we have observed that motoneurons from rat spinal cord embryonic explants, growing on plates covered with polyornithine and laminin, have the singularity of migrating outside the spinal cord, and grow as a monolayer of cells surrounded by glial cells. This system offers some advantages for the individual study of these motoneurons. In this new model, we have assessed the interaction between the proinflammatory cytokines TNF-α and IFN-γ on microglial activation, NO and oxidative stress generation and, importantly, the functional implications on the viability of spinal cord motoneurons.

EXPERIMENTAL PROCEDURES

Materials

Rat and murine IFN-γ or TNF-α was purchased from PeproTech EC Ltd. (London, UK). The selective iNOS inhibitor 4H-1,3-thiazin-2-amine, 5,6-dihydro-6-methyl-hydrochloride [AMT] was from Cayman Chemical (Ann Arbor, MI, USA). Other reagents were from Sigma-Aldrich (St. Louis, MO, USA), except when indicated.

Rat spinal cord embryonic explants and cytokine treatments

Embryos at gestational age of 15–16 days (E15-16) were removed by cesarean section from pregnant Sprague–Dawley rats (Charles River, Barcelona, Spain). Lumbar spinal cords were dissected from each embryo with forceps, transferred to ice cold Leibowitz's 15 medium (L15) and the meninges and ganglia carefully removed. Cords were transversely sectioned into 350-μm slices with a MacIlwain tissue chopper (Gomshall, Surrey, UK). Sections were carefully placed at a density of 20 sections per well on 35 mm-wells precoated with poly-DL-ornithine (30 μg/ml) and L-laminin (2 μg/ml) and containing 2 ml of Eagle's minimal essential medium (MEM) supplemented with 5% heat-inactivated horse serum, 5% fetal bovine serum, 2 mM glutamine, 0.6% glucose and 15 μg/ml gentamicin. Explants were maintained at 37 °C under a humidified 5% CO_2 atmosphere. To avoid the detachment of explants the wells were not manipulated during the first 4 days after platting; then, medium was changed and thereby every 3 days. After 5 days *in vitro*, some cells of the spinal cord, including motoneurons, started the migration outside the explant (Fig. 1). All treatments started 10 days after the explant procedure.

Where indicated, rat spinal cord embryonic explants were exposed for 48 h to IFN-γ (10 ng/ml), TNF-α (10 ng/ml) or both cytokines together, in the presence or absence of the selective iNOS and nicotinamide adenine dinucleotide phosphate (NADPH) oxidase inhibitors, AMT (10 μM) and apocynin (1 mM), respectively. The time of exposure and the concentration of the cytokines were chosen based on our previous work demonstrating microglial activation, iNOS induction and NO generation with these particular conditions (Mir et al., 2008), and other studies (He et al., 2002; Mander and Brown, 2005; Gibbons and Dragunow, 2006).

Immunohistochemistry

The following primary antibodies were used for immunohistochemistry: anti–microtubule-associated protein 2 (MAP2) (1:1000) from Chemicon (Temecula, CA, USA); SMI-32 (1:1000) from Abcam plc (Cambridge, UK); anti-Islet1 (40.2D6, 1:200) from Developmental Studies Hybridoma Bank (Iowa City, IA, USA); anti–vesicular acetylcholine transporter (VAChT) (1:500) from Synaptic Systems (Göttingen, Germany); anti-iNOS (1:200) from BD Biosciences (Franklin Lakes, NJ, USA); anti-active caspase-3 (1:200) from Cell Signaling Technology (Danvers, MA, USA); anti-nitrotyrosine (1:750) from Upstate (Charlottesville, VA, USA) and anti–glial fibrillary acidic protein (anti-GFAP; 1:1000) from DAKO (Glostrup, Denmark). For lectin cytochemistry, the lectin from *Lycopersicon esculentum* (tomato lectin) labeled with fluorescein isothiocyanate (FITC) (25 μg/ml) was used.

Rat spinal cord embryonic explants were exposed to cytokines as indicated and then fixed with 4% paraformaldehyde in 0.1 M phosphate buffer, pH 7.4 for 30 min at 21±1 °C. Explants were permeabilized for 5 min with methanol, washed three times with Tris buffer saline (TBS), pH 7.4 and then blocked in 0.1% Triton X-100, 5% normal horse serum (NHS) in TBS for 1 h. For active caspase-3 immunohistochemistry, 0.4% Triton X-100 and 20% NHS were used for permeabilization and blocking, respectively. Explants were then incubated overnight at 4 °C with one or two of the above primary antibodies. Immunohistochemical controls, performed by omitting the primary antibody, resulted in the abolition of the immunostaining. For immunofluorescence, sections were incubated for 1 h with the appropriate secondary antibody, Alexa Fluor 555 goat anti-rabbit IgG (1:200), Alexa Fluor 488 goat anti-mouse IgG (1:200) or Alexa Fluor 350 goat anti-mouse IgG (1:200) (Invitrogen, Carlsbad, CA, USA). Cultures were then washed and mounted using Gelmount solution. In some cases of immunohistochemistry the secondary antibody used was a biotinylated goat–antimouse and explants were processed according to the standard avidin–biotin complex procedure (Vector Laboratories, Burlingame, CA, USA); the diaminobenzidine (DAB) reaction was used for color development.

For co-localization of SMI-32 and Islet1-positive neurons, explants were first incubated with Islet1 antibody, followed by incubation with biotinylated goat anti-mouse antibody and processed for the DAB reaction as described above. After incubating with avidin/biotin blocker (Vector Laboratories) to saturate all free avidin or biotin residues, explants were then reprobed with SMI-32 antibody followed by incubation with Alexa Fluor 488 goat anti-mouse IgG. Because both SMI-32 and Islet1 are monoclonal antibodies, goat anti-mouse antibodies applied after SMI-32 incubation may also react with Islet1-positive cells. To test the specificity of the secondary antibody against SMI-32, the second primary antibody (SMI-32) was omitted; in this case, no green fluorescence was detected (not shown), indicating that there was no cross-reactivity.

Images were obtained using a Leica DMR epifluorescence microscope (Leica Microsystems, Wetzlar, Germany) equipped with a Leica DC300 camera and software. Some samples were also imaged under a Leica TCS SP2 confocal laser scanning microscope.

Quantification of apoptotic motoneuron death

To assess whether a given cytokine treatment affected the viability of motoneurons, its ability to induce apoptotic cell death was monitored by means of the APOAC annexin V-Cy3 apoptosis detection kit (Sigma-Aldrich); this kit detects the presence of phosphatidylserine residues on the outer leaflet of the plasma membrane by means of the protein annexin conjugated to the fluoro-

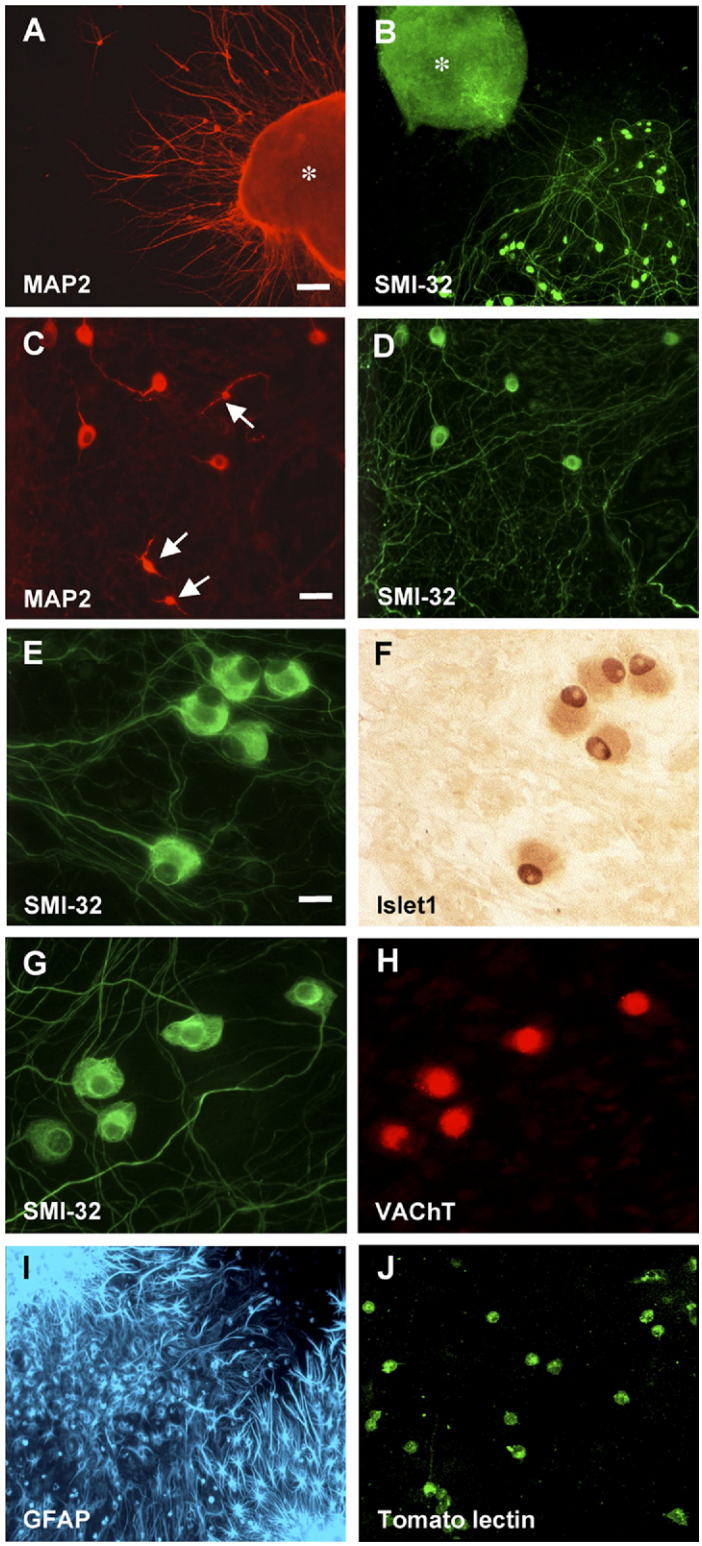

Fig. 1. Migration of cells from rat spinal cord embryonic explants. (A) Immunohistochemistry for MAP2 in a rat spinal cord embryonic explant after five days *in vitro* showing interneurons in the process of migration outside the explant. (B) Immunohistochemistry for SMI-32 in an explant after seven days *in vitro* showing motoneurons in the process of migration outside the ventral side of the spinal cord. * Indicates the location of the explant in (A) and (B). (C, D) Immunohistochemistry for (C) MAP2 and (D) SMI-32 showing that motoneurons are co-labeled with MAP2 and SMI-32 antibodies, and that interneurons are positive for MAP2 (arrows) but are not labeled with the SMI-32 antibody. (E–H) Identification of motoneurons in rat spinal cord embryonic explants after 10 days *in vitro* by dual labeling using (E) SMI-32 and (F) Islet1 antisera with fluorescein and DAB staining, respectively and by using (G) SMI-32 and (H) VAChT antisera. Note the co-localization of SMI-32 with Islet1 and with VAChT immunoreactivities. (I, J) Immunofluorescence for (I) GFAP and (J) tomato lectin in rat spinal cord embryonic explants after 10 days *in vitro* showing (I) astrocytes and (J) microglial cells that have migrated outside the explant. Scale bars=80 μm (A), also applies to (B). (C) Forty micrometers, also applies to (D) and (I). (E) Twenty micrometers also applies to (F), (G), (H) and (J).

chrome Cy3.18 (Koopman et al., 1994). Briefly, explants were rinsed with phosphate-buffered saline (PBS), pH 7.4 at 37 °C for 10 min, and then exposed to annexin V-Cy3 (1 μg/ml) in the binding buffer supplied by the manufacturer. Then, explants were rinsed again with PBS and processed for SMI-32 immunofluorescence. The percentage of motoneurons undergoing apoptotic cell death was assessed by counting the number of annexin V-Cy3 positive cells that could be identified as motoneurons both by morphological and immunocytochemical criteria (i.e. double labeled with annexin V-Cy3 and SMI-32), relative to the total number of motoneurons (SMI-32 positive) in the whole area of the well. Only motoneurons with their somata out of the explant were counted. The mean number of counted motoneurons in control wells was 78±7 (n=20). Cell counts were done blindly as to the treatment condition and at least three different wells were counted for each experimental condition. The procedure described here for the quantification of annexin V positive motoneurons also applies for the quantification of active caspase-3 and nitrotyrosine positive motoneurons after the indicated experimental treatments.

Western blotting

Rat spinal cord embryonic explants were exposed to cytokines as indicated and, after treatments, explants were rinsed rapidly in ice cold PBS and lysed in 2% sodium dodecyl sulfate (SDS), 125 mM Tris buffer, pH 6.8 containing a cocktail of protease inhibitors (Complete Mini; Roche Pharmaceuticals, Basel, Switzerland). Lysates were sonicated and proteins quantified by means of the DC Protein Assay from Bio-Rad Laboratories (Hercules, CA, USA). Protein equivalents from each sample were resolved in SDS–polyacrylamide gel electrophoresis and electrotransferred to 0.45 μm nitrocellulose membranes (Amersham, Buckinghamshire, UK) using a Bio-Rad semidry trans-blot, according to the manufacturer's instructions. Membranes were blocked at 21±1 °C for 1 h with PBS containing 5% non-fat dry milk, 0.5% bovine serum albumin (BSA) and 0.2% Tween 20. Membranes were probed overnight at 4 °C with the adequate primary antibodies: anti-iNOS (1:4000) or anti–cyclooxygenase-2 (anti-COX-2; 1:2000) from Cayman Chemical Company; anti-gp91^{phox} (1:2000) or anti-α-tubulin (1:10,000) from Sigma-Aldrich. Membranes were then washed with PBS for 10 min at 21±1 °C (three times) and incubated for 2 h with the appropriate peroxidase-conjugated secondary antibodies. These antibodies were used at the dilutions recommended by the suppliers. Blots were finally developed with the chemiluminescent peroxidase substrate and visualized in chemiluminescence film (Amersham). The apparent molecular weight of proteins was determined by calibrating the blots with pre-stained molecular weight markers (Bio-Rad).

NO determination in culture medium

Rat spinal cord embryonic explants were exposed for 48 h to IFN-γ (10 ng/ml), TNF-α (10 ng/ml) or both cytokines together in the presence or absence of the selective iNOS inhibitor AMT. NO produced by the explants was determined in culture media by assaying the amount of nitrite, a stable oxidation product of NO, using the Griess reagent (Green et al., 1982), as previously described (Mir et al., 2008).

Nuclear factor kappa B (NF-κB) activity measurements

NF-κB activation was assessed in rat spinal cord embryonic explants exposed for 24 h to IFN-γ (10 ng/ml), TNF-α (10 ng/ml) or both cytokines together by means of the NF-κB transcription factor Assay Kit (TransAMTM) from Active Motif, as previously described (Mir et al., 2008). Briefly, explants cultured in four 35 mm-wells were collected and mixed for every treatment to perform the assay. Nuclear extracts were prepared and incubated with an immobilized oligonucleotide containing an NF-κB consensus binding site. The NF-κB complex bound was then detected with an antibody against an epitope of the p65 (RelA) subunit of NF-κB, followed by incubation with the adequate peroxidase-conjugated secondary antibody and with a developing solution.

Protein carbonyl measurement

Oxidative damage of rat spinal cord embryonic explants was determined after exposure for 48 h to IFN-γ (10 ng/ml), TNF-α (10 ng/ml), or both cytokines together, by measuring the content of protein carbonyl as determined by the 2,4-dinitrophenylhydrazine (DNPH) spectrophotometric assay. In this assay, DNPH reacts with protein carbonyls, forming a Schiff base to produce the corresponding hydrazone, which can be analyzed spectrophotometrically (Levine et al., 1994). Embryonic explants cultured in four 35 mm-wells were collected and mixed for every treatment to perform the assay. Explants were scraped and sonicated on ice in 500 μl of cold 50 mM sodium phosphate buffer pH 6.7 containing 1 mM EDTA and a cocktail of protease inhibitors (Complete Mini; Roche Pharmaceuticals), and homogenates centrifuged at 10,000×g for 15 min at 4 °C. Supernatants were collected and the ratio of absorbances 280/260 nm was checked to be more than 1, as nucleic acids may erroneously contribute to a higher estimation of carbonyls. Total protein content in the supernatants was measured by means of the DC Protein Assay from Bio-Rad Laboratories. The supernatant fraction was divided in two 200 μl aliquots, one sample was treated with 800 μl DNPH and the other sample with an equal volume of 2.5 M HCl. Both samples were incubated in the dark at 21±1 °C for 1 h and vortex-mixed at 15-min intervals. Both aliquots were precipitated on ice for 5 min with 1 ml of 20% (wt/vol) trichloroacetic acid and then centrifuged at 10,000×g for 10 min at 4 °C. Supernatants were then reprecipitated with 10% trichloroacetic acid and centrifuged as above. The precipitates were washed three times with ethanol/ethyl acetate (1:1 vol/vol) and the final pellet was dissolved in 6 M guanidine HCl in 20 mM sodium phosphate buffer, pH 6.7. Insoluble debris was removed by centrifugation as above. The difference spectrum of the DNPH-treated sample versus the HCl control was determined, and the results were expressed as nanomoles of DNPH incorporated per milligram of protein, based on the absorption of 21.0 mM^{-1} cm^{-1} at 375 nm for aliphatic hydrazones.

Mouse motoneurons isolation and quantification of cell survival

Motoneurons were purified from mouse embryos by optimizing different steps of protocols described for chicken (Soler et al., 1998) and mouse motoneurons (Arce et al., 1999) isolation. Briefly, mouse embryo (E12.5) spinal cords were dissected and the dorsal half was removed. Ventral cords were chopped into pieces and incubated for 10 min at 37 °C in GHEBS buffer (137 mM NaCl, 2.7 mM KCl, 22.2 mM glucose, 25 mM Hepes buffer pH 7.4 and 20 IU/ml penicillin plus 20 μg/ml streptomycin) containing 0.025% trypsin. Then cords were mechanically dissociated and collected under a 4% BSA cushion. The largest cells were then isolated by centrifugation (10 min at 520×g) on an OptiPrep (iodixanol) (Axis-Shield plc, Dundee, Scotland) density gradient. At the end of this procedure, cells were again centrifuged through a BSA cushion. The collected cells were pooled in a tube containing culture medium, counted with a hemocytometer and plated on four-well culture dishes (Falcon, BD Biosciences) precoated with poly-DL-ornithine and L-laminin at a density of 1250 cells per well. Culture medium was Neurobasal (GIBCO, Invitrogen) supplemented with the B27 supplement (GIBCO, Invitrogen), 2% horse serum, 0.5 mM L-glutamine, 25 μM 2-mercaptoethanol and the recombinant neurotrophic factors: brain-derived neurotrophic fac-

tor (BDNF) (1 ng/ml), glial cell line-derived neurotrophic factor (GDNF) (10 ng/ml), ciliary neurotrophic factor (CNTF) (10 ng/ml), cardiotrophin-1 (CT-1) (10 ng/ml) and hepatocyte growth factor (HGF) (10 ng/ml) (PeproTech EC Ltd.).

For survival experiments, motoneurons were exposed for 48 h to TNF-α (10, 50 or 100 ng/ml), IFN-γ (10, 50 or 100 ng/ml), or both cytokines together. The expression of receptors for proinflammatory cytokines in spinal cord motoneurons at E12.5 gestational age has already been reported (Sedel et al., 2004). Quantification of motoneuron survival was performed by counting the number of large phase-bright neurons with long axonal/neurite processes in the whole area of the well. The percentage of surviving cells in the different conditions studied was normalized with respect to the number of cells present in control (non-treated) cultures. Motoneurons cultured for 48 h in supplemented Neurobasal medium but in the absence of neurotrophic factors were taken as a negative control of cell survival. The mean number of counted motoneurons in control wells was 172 ± 8 ($n=9$). Cell counts were done blindly as to the treatment condition and at least three different wells were counted for each experimental condition.

Statistics

All experiments were repeated at least three times. Data are expressed as mean$\pm$SEM values. One-way analysis of variance (ANOVA) followed by Bonferroni test was used for the statistical evaluations. Differences were considered significant when the P-value was <0.05.

RESULTS

Characterization of migrating motoneurons in rat spinal cord embryonic explants

We observed that in rat spinal cord embryonic explants after five days *in vitro* growing on plates covered with polyornithine and laminin, some cells started the migration outside the explant. Neurons, identified by anti-MAP2, migrated from different points around the spinal cord (Fig. 1A). Motoneurons were first identified by anti–neurofilament heavy chain (NF-H, SMI-32) immunostaining and on the basis of their morphology: large bodies (>20 μm) of rounded or triangular shape with a single well-defined axon (see also De Paola et al., 2008); these SMI-32-positive cells started the migration from the ventral side of the spinal cord (Fig. 1B). The SMI-32-positive population could also be labeled with the anti-MAP2 antibody (Fig. 1C, D), however, the spinal cord interneurons, positive for MAP-2, were not positive for the SMI-32 antibody (Fig. 1C, D). After 10 days *in vitro*, motoneurons appeared forming groups growing in monolayers outside the explant (Fig. 1E). To further confirm that these cells corresponded to motoneurons, the co-localization of SMI-32 with Islet1, a LIM homeodomain transcription factor assumed to be expressed specifically by motoneurons (Yamada et al., 1993; Tsuchida et al., 1994; Francisco-Morcillo et al., 2006) and with the cholinergic marker VAChT (Wetts et al., 2001; Härtig et al., 2007) was assessed. Migrating cells with large cell bodies and SMI-32 positive were found to be labeled both by the Islet1 (Fig. 1E, F) and by the VAChT antibody (Fig. 1G, H); thus indicating that the SMI-32-positive population corresponded to spinal cord motoneurons. Other migrating cells were identified as astrocytes as well as microglia by means of GFAP (Fig. 1I) and tomato lectin (Fig. 1J) immunohistochemistry, respectively.

TNF-α and IFN-γ cooperate in iNOS, gp91^{phox} and COX-2 expression via NF-κB in rat spinal cord embryonic explants

The expression of the iNOS enzyme was assessed in rat spinal cord embryonic explants after different cytokine treatments. In control explants, low expression of iNOS was detected; however, exposure to IFN-γ (10 ng/ml), but not TNF-α (10 ng/ml), significantly increased iNOS expression (Fig. 2A). In agreement with our previous study in pure microglial cultures (Mir et al., 2008), when explants were exposed to both cytokines together, iNOS expression was clearly increased in comparison with IFN-γ alone (Fig. 2A). This result was confirmed by measuring NO production in culture media. The levels of nitrite, an oxidation product of NO, were consistent with the expression levels of iNOS after the different cytokine treatments (i.e. the maximal nitrite levels were obtained in the presence of TNF-α and IFN-γ). The selective iNOS inhibitor AMT blocked NO production stimulated by the combination of both cytokines (Fig. 2B). To assess which cell of the spinal cord explants expressed iNOS in response to the cytokines, immunohistochemistry co-localization experiments were performed and showed that, after exposure to TNF-α and IFN-γ, the increase in iNOS expression occurred specifically in microglia (Fig. 2D), but not in astroglia (Fig. 2E).

The transcription factor NF-κB plays a key role in iNOS gene induction, and we have previously demonstrated that TNF-α and IFN-γ cooperate in iNOS gene expression through increased NF-κB activation in microglia (Mir et al., 2008). To assess the mechanism underlying the cooperative effect between the two cytokines on iNOS expression and NO production; experiments were performed in which NF-κB binding to DNA was studied in nuclear extracts obtained from explants exposed to TNF-α, IFN-γ or both cytokines together. In agreement with our previous study (Mir et al., 2008), both TNF-α and IFN-γ were able to induce NF-κB activation above the basal levels; however, when cells were challenged with both cytokines together, a significant increase in NF-κB binding to DNA was observed, as compared to the effect of each cytokine alone (Fig. 2C). On the basis of the observation of iNOS expression, we postulated that TNF-α and IFN-γ might also cooperatively regulate the transcription of other genes also containing κB motifs. Therefore, the expression of the catalytic subunit of the NADPH oxidase, gp91^{phox} (otherwise known as Nox2) (Gauss et al., 2007) and the lipid-oxidizing enzyme COX-2 (Nakao et al., 2002) were studied. As shown in Fig. 2A, these enzymes were induced by TNF-α but not by IFN-γ; however, and importantly to our study, when both cytokines were added together an increase in the expression levels of both gp91^{phox} and COX-2 was clearly detected. Together, these results indicated that TNF-α and IFN-γ cooperate, via the transcription factor NF-κB, to increase the expression of oxidative stress-inducing enzymes.

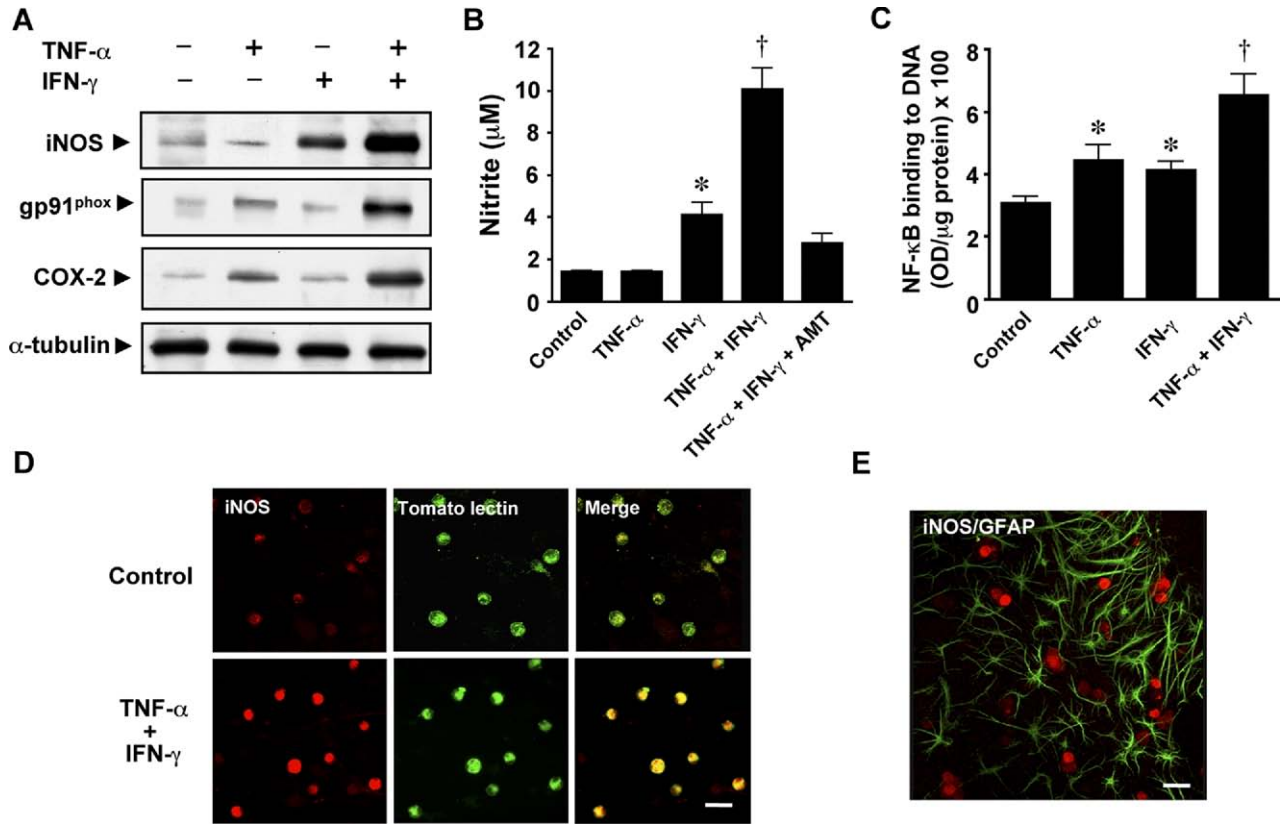

Fig. 2. TNF-α and IFN-γ cooperate in iNOS, gp91^{phox} and COX-2 expression via NF-κB. Rat spinal cord embryonic explants were exposed for 48 h to TNF-α or IFN-γ (both at 10 ng/ml) alone or in combination, as indicated. (A) Western blots showing iNOS, gp91^{phox} and COX-2 immunoreactivities in lysates (15 μg of protein) of rat spinal cord embryonic explants after the indicated treatments. α-Tubulin immunoreactivity is shown as a control of total protein loaded per lane. A representative immunoblot of three independent experiments is shown. (B) Amounts of NO in culture media of rat spinal cord embryonic explants after the indicated treatments by measuring nitrite using the Griess reagent. The selective inhibitor of iNOS AMT (10 μM) was used as a negative control to block NO production when indicated. Columns represent the mean±SEM of six independent experiments with three wells for experimental condition. * $P<0.01$ as compared to control (untreated) and to explants exposed to TNF-α and † $P<0.001$ as compared to the other experimental paradigms (ANOVA followed by Bonferroni test). (C) Rat spinal cord embryonic explants were exposed for 24 h to TNF-α or IFN-γ (both at 10 ng/ml) alone or in combination, as indicated, and nuclear extracts prepared and assayed for NF-κB activity as described in Experimental Procedures. Columns represent values of optical density (OD) corrected by the micrograms of total nuclear proteins in the extract and are the mean±SEM of three independent experiments with four wells for experimental condition. * $P<0.05$ as compared to control (untreated) explants and at least † $P<0.01$ as compared to the other experimental paradigms (ANOVA followed by Bonferroni test). (D) Immunohistochemistry for iNOS in rat spinal cord embryonic explants after the indicated treatments. The explants were also labeled with tomato lectin to show microglial cells. iNOS shows co-localization with tomato lectin (merge). (E) Double immunohistochemistry for iNOS (red) and GFAP (green) in rat spinal cord embryonic explants exposed to TNF-α and IFN-γ. Scale bars=20 μm, applies to all photographs in (D) and (E).

TNF-α and IFN-γ cooperate in inducing oxidative stress in rat spinal cord embryonic explants

Total protein carbonyl content after exposure to the cytokines TNF-α and IFN-γ was examined in rat spinal cord embryonic explants to assess the extent of oxidative free radical damage to proteins. When explants were exposed for 48 h to TNF-α or IFN-γ (both at 10 ng/ml) a significant increase in carbonyl levels as compared to control (untreated) explants was observed. The levels of protein carbonyl content were significantly higher in the explants exposed to IFN-γ than in those exposed to TNF-α (Fig. 3A). When the above cytokines were added in combination a further and significant increase in oxidized proteins was observed (Fig. 3A).

iNOS and NADPH oxidase produce NO and superoxide (O_2^-), respectively, which combine by a diffusion-limited reaction to form the more toxic oxidant peroxynitrite ($ONOO^-$); this anion, in turn, can nitrate tyrosine groups of proteins and forms the stable compound 3-nitrotyrosine. Thus, nitrotyrosine immunoreactivity can be used as an indicator of NO and superoxide production (Dawson and Dawson, 1998). When explants were exposed for 48 h to TNF-α or IFN-γ a significant increase in the percentage of motoneurons (SMI-32 positive) that were also nitrotyrosine positive was detected. However, exposure of explants to IFN-γ resulted in a higher percentage of nitrotyrosine positive motoneurons than in those exposed to TNF-α (Fig. 3B). Interestingly, and in accordance with the previously described effects of TNF-α and IFN-γ on NO production, when explants were exposed to both cytokines together, this percentage was significantly increased in comparison with each cytokine alone (Fig. 3B, C). Moreover, immunohistochemistry for SMI-32 showed shrunken somata and condensed cytoskeleton in motoneurons treated with

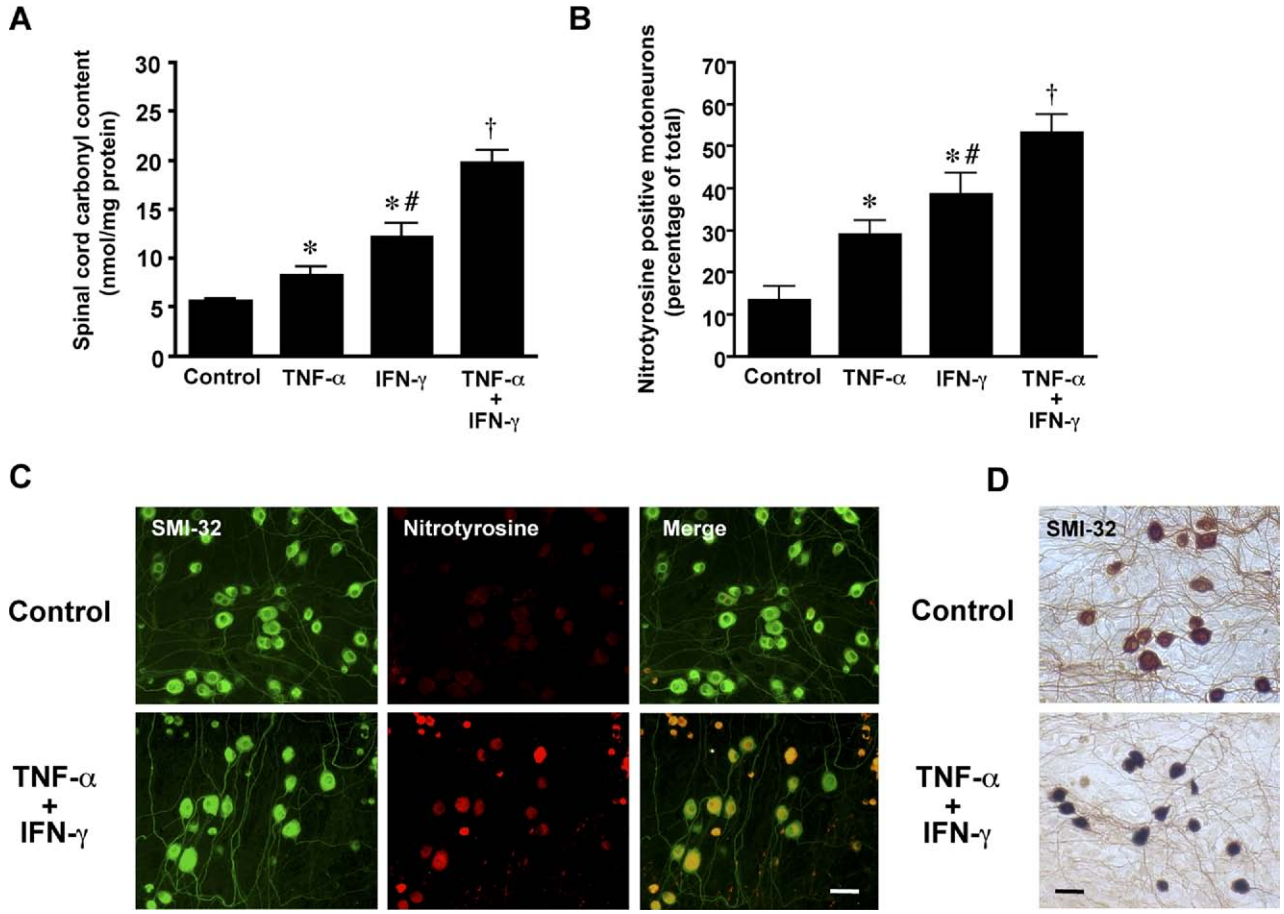

Fig. 3. TNF-α and IFN-γ cooperate in inducing oxidative stress in rat spinal cord embryonic explants. Rat spinal cord embryonic explants were exposed for 48 h to TNF-α or IFN-γ (both at 10 ng/ml) alone or in combination, as indicated. (A) Levels of protein carbonyl content of oxidatively modified proteins measured in explants after the indicated treatments by the DNPH spectrophotometric assay. Columns represent the mean±SEM of three independent experiments with four wells for experimental condition. At least * $P<0.05$ as compared to control (untreated) explants, # $P<0.01$ as compared to explants exposed to TNF-α and at least † $P<0.01$ as compared to the other experimental paradigms (ANOVA followed by Bonferroni test). (B) Quantification of nitrotyrosine positive motoneurons as described in Experimental Procedures in rat spinal cord embryonic explants treated as indicated. Columns represent the mean±SEM of six independent experiments with three wells for experimental condition. At least * $P<0.05$ as compared to control (untreated) explants, # $P<0.01$ as compared to explants exposed to TNF-α and at least † $P<0.01$ as compared to the other experimental paradigms (ANOVA followed by Bonferroni test). (C) Representative immunofluorescence images of rat spinal cord embryonic explants treated as indicated and double-labeled with SMI-32 and anti-nitrotyrosine. (D) Representative immunohistochemistry for SMI-32 (DAB reaction) in rat spinal cord embryonic explants treated as indicated. Scale bars=40 μm; applies to all photographs in (C) and (D).

TNF-α and IFN-γ, as compared to control (untreated) cells, suggesting that the viability of spinal cord motoneurons was compromised after exposure to these cytokines (Fig. 3C, D).

TNF-α and IFN-γ cooperate in inducing apoptotic motoneuron death

It has been demonstrated that when the rat spinal cord is exposed to peroxynitrite, it induces neuronal apoptotic cell death together with caspase-3 activation (Bao and Liu, 2003); and also that free nitrotyrosine exposure induces apoptotic motoneuron death (Peluffo et al., 2004). Thus, the potential effects of the cytokines TNF-α and IFN-γ inducing apoptotic motoneuron death were studied. As shown in Fig. 4A, when rat spinal cord embryonic explants were exposed for 48 h to TNF-α or IFN-γ (both at 10 ng/ml), a significant increase in the percentage of motoneurons (SMI-32 positive) that were also annexin V positive was detected. Exposure to IFN-γ resulted in a higher percentage of annexin V positive motoneurons as compared to TNF-α alone (Fig. 4A). Interestingly, when explants were exposed to both cytokines together, this percentage of motoneurons significantly increased in comparison with each cytokine alone (Fig. 4A, B), and this effect could be completely abolished in the presence of the selective iNOS inhibitor AMT (10 μM) or in the presence of the selective NADPH oxidase inhibitor apocynin (1 mM) (Fig. 4A). To further assess that the increase in annexin-Cy3 immunofluorescence indicated an early event of the apoptotic pathway, the activation of the executioner caspase-3 was studied in explants exposed to TNF-α and IFN-γ. A significant increase in the percentage of motoneurons that were positive for active caspase-3 was detected as compared to control cells in these explants (Fig. 4C, D).

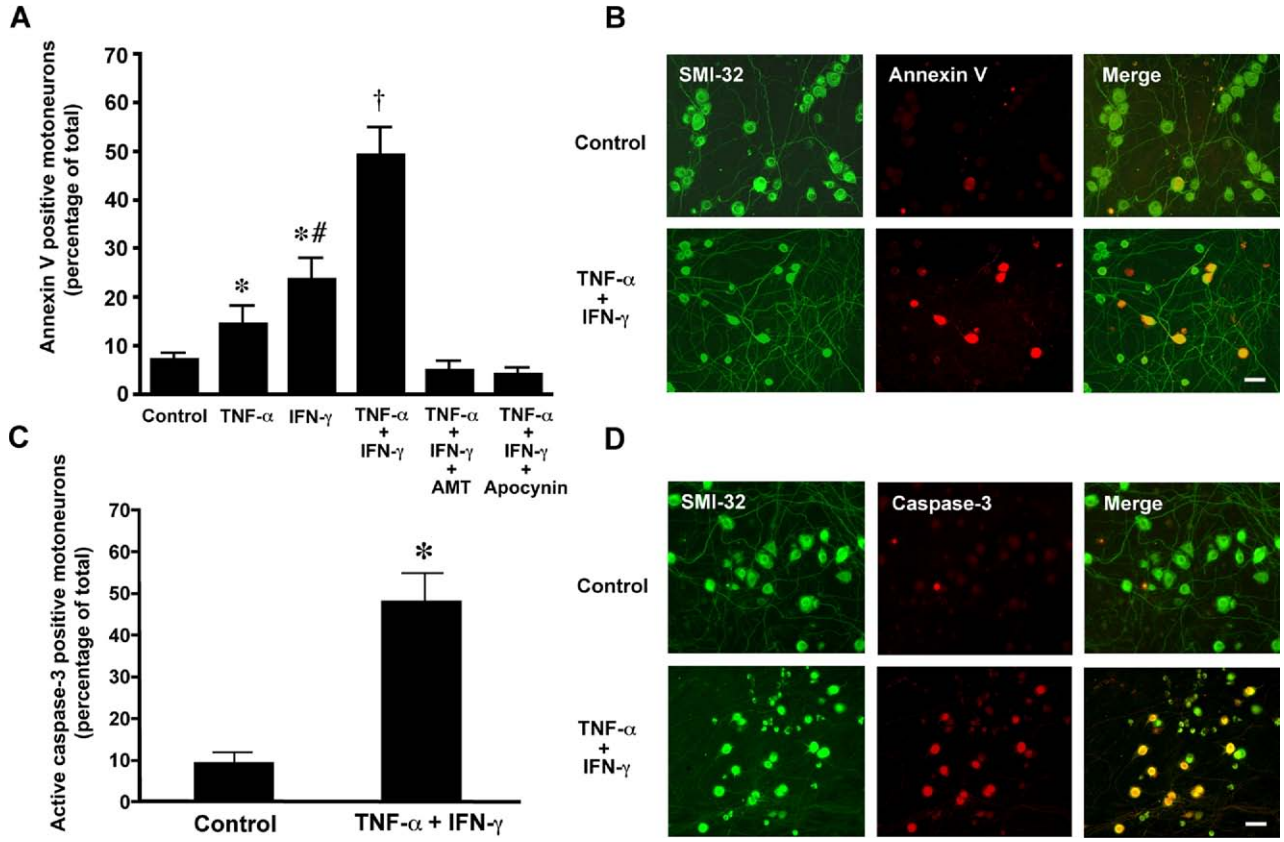

Fig. 4. Cooperative induction of apoptotic motoneuron death by TNF-α and IFN-γ. Rat spinal cord embryonic explants were exposed for 48 h to TNF-α or IFN-γ (both at 10 ng/ml) alone or in combination and, in this case, in the absence or presence of the selective inhibitor of iNOS AMT (10 μM) or the selective NADPH inhibitor apocynin (1 mM), as indicated. (A) Quantification of apoptotic motoneuron death by labeling them with annexinV-Cy3 as described in Experimental Procedures. Columns represent the mean±SEM of six independent experiments with three wells for experimental condition. At least * $P<0.05$ as compared to control (untreated) explants, # $P<0.01$ as compared to explants exposed to TNF-α and at least † $P<0.01$ as compared to the other experimental paradigms (ANOVA followed by Bonferroni test). (B) Representative immunofluorescence images of rat spinal cord embryonic explants treated as indicated and double-labeled with SMI-32 and annexin V-Cy3. (C) Quantification of active caspase-3 positive motoneurons as described in Experimental Procedures in rat spinal cord embryonic explants treated as indicated. Columns represent the mean±SEM of three independent experiments with three wells for experimental condition. * $P<0.001$ as compared to control (untreated) explants (Student's *t*-test). (D) Representative immunofluorescence images of rat spinal cord embryonic explants treated as indicated and double-labeled with SMI-32 and anti-active caspase-3. Scale bars=40 μm, applies to all photographs in (B) and (D).

Interestingly, the percentage of motoneurons positive for active caspase-3 matched the percentage of annexin V positive motoneurons found after exposure to the cytokine combination (Fig. 4A, C). Together, these results indicated that the proinflammatory cytokines TNF-α and IFN-γ cooperate to induce apoptotic cell death in spinal cord motoneurons.

TNF-α and IFN-γ do not affect the viability of purified spinal cord motoneurons

To further confirm that the presence of activated microglia and the increased oxidative stress after exposure to the proinflammatory cytokines TNF-α and IFN-γ may be involved in inducing motoneuron death, a culture of purified spinal cord motoneurons was used. In this culture, motoneurons exposed for 48 h to TNF-α or IFN-γ alone or in combination, at the concentrations employed in the rat spinal cord embryonic explant, i.e. 10 ng/ml, appeared similar to untreated cultures based on cell morphology; in addition, no variation in the number of surviving motoneurons was observed (not shown). Thereafter, the concentration of the cytokines was increased to 50 and 100 ng/ml; however, no effects could be observed in the parameters described above after treatments with TNF-α or IFN-γ at these high cytokine concentrations (Fig. 5A, B). Thus, these results indicated the lack of toxicity of these cytokines on spinal cord motoneurons in the absence of glial cells.

DISCUSSION

Several models have been developed for the *in vitro* study of the functionality of spinal cord motoneurons in the presence of glial cells. The rat organotypic spinal cord culture preserves the *in vivo* horizontal architecture; however, in this model, the detailed microscopic study of motoneurons is limited by the thickness of the spinal cord sections (Rothstein et al., 1993; Tolosa et al., 2008). The dissociated spinal cord culture works with overall embryonic cords

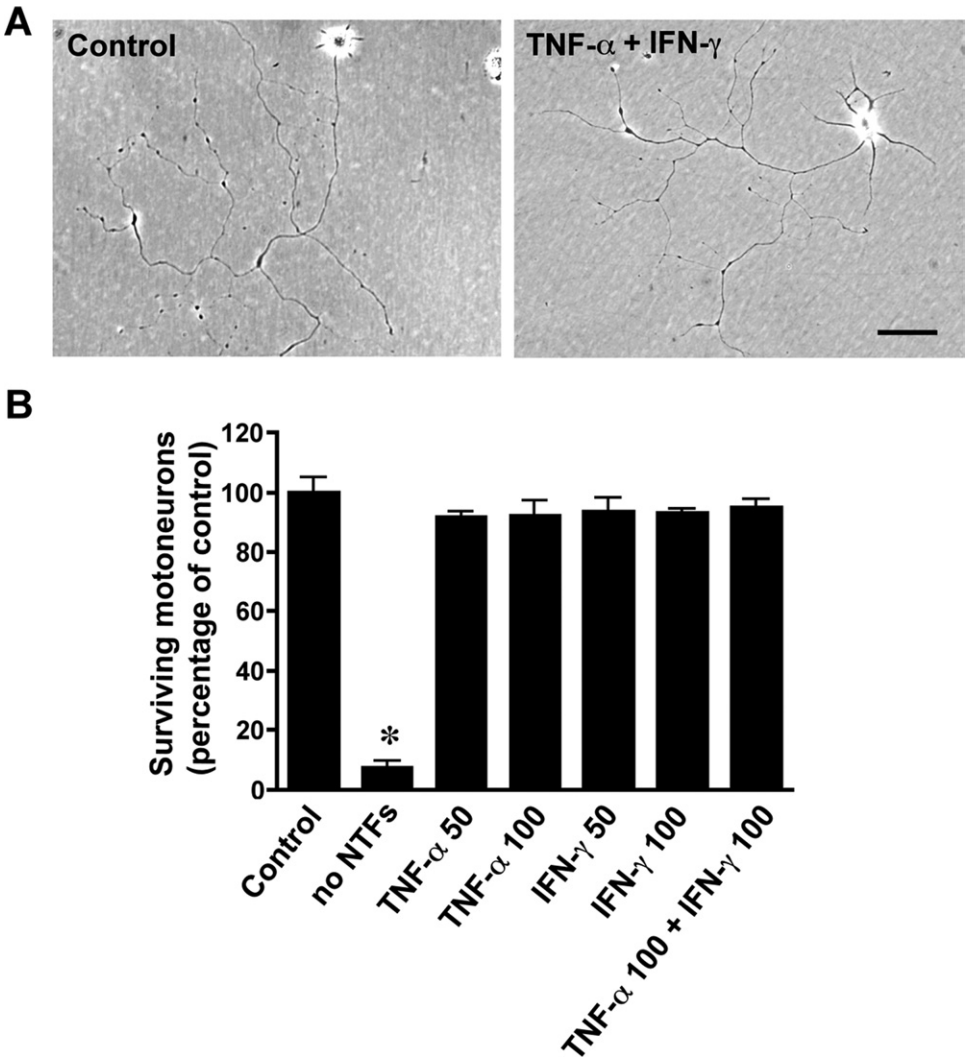

Fig. 5. Lack of effects of TNF-α and IFN-γ on the viability of purified motoneurons. (A) Photomicrograph using phase-contrast microscopy of control (untreated) or exposed for 48 h to TNF-α and IFN-γ (both at 100 ng/ml) spinal cord motoneurons from mouse embryos. The motoneurons were isolated by centrifugation on an OptiPrep density gradient. (B) Quantification of motoneuron viability after the different indicated treatments as described in Experimental Procedures. Motoneurons cultured in the absence of neurotrophic factors (no NTFs) were taken as negative control of cell survival. Columns represent the mean±SEM of three independent experiments with three wells for experimental condition. * $P<0.001$ as compared to control (untreated) cultures. Scale bar=30 μm, applies to both photographs.

and the tissue is separated mechanically by repeated trituration. In this model, the efficiency, i.e. the final number of cultured motoneurons per well is rather small (Bar-Peled et al., 1999). Here, we present a new culture system for spinal cord motoneurons in the presence of glial cells; this model is based on that embryonic motoneurons and other spinal cord cells migrate outside the explant (Fig. 1), and the main advantage is that motoneurons appear forming monolayers surrounded by glial cells; this fact allows for the detailed microscopic study of motoneurons and, probably, for other techniques such as electrophysiology. In addition, as the tissue has not been mechanically triturated, the efficiency of this model, in terms of the final number of cultured motoneurons, is very high. In the present work we have not investigated the process of migration of motoneurons; however, in chick embryos it has been demonstrated that motoneuron somata are confined to the CNS by interactions with the so-called boundary cap cells (a neural crest subpopulation present in the motor exit points). The surgical elimination of these cells results in motoneuron migration out of the spinal cord (Vermeren et al., 2003). Thus, it can be proposed that, in our model, migration of motoneuron somata from the spinal cord occurs through motor exit points that have been disrupted when lumbar spinal cords were removed and sectioned.

The proinflammatory cytokines TNF-α and IFN-γ have been proposed to be involved in ALS-linked microglial activation (He et al., 2002; Sargsyan et al., 2005; Wen et al., 2006), thus suggesting a rationale for their application in our culture model. The present results demonstrating cooperative effects of TNF-α and IFN-γ on iNOS expres-

sion and NO production (Fig. 2A, B) are in agreement with those previously obtained in pure cultures of microglial cells (Mir et al., 2008). In these cultures, we demonstrated that the cooperative effects of TNF-α and IFN-γ on microglial iNOS expression relied in part on their cooperative effects on NF-κB and interferon regulatory factor-1 (IRF-1) activation, two key transcription factors regulating iNOS gene expression (Mir et al., 2008). As similar results on NF-κB activation were obtained when explants were exposed to the above cytokines (Fig. 2C) and iNOS was mainly induced in microglia (Fig. 2D), but not in astroglia (Fig. 2E), the same mechanisms described in pure microglial cultures may be claimed for the cooperative effects of TNF-α and IFN-γ on iNOS expression found in our explants. Interestingly, in spinal cords of ALS patients iNOS immunoreactivity was also found increased; however, it was observed mainly in reactive astrocytes (Sasaki et al., 2000). The discrepancy with our results may be due to the short-term period (48 h) of exposure to cytokines; thus, microglia may respond earlier to TNF-α and IFN-γ than astroglia. iNOS has also been found up-regulated in glial cells of the spinal cord of early symptomatic and end-stage transgenic mutant SOD1 mice and the time course of iNOS up-regulation paralleled that of motoneuron loss (Almer et al., 1999). Also in this sense, NO produced by lipopolysaccharide (LPS)-activated microglia has been shown to be implicated in motoneuron injury (Zhao et al., 2004).

Superoxide is produced by the microglial enzyme NADPH oxidase, also known as phagocytic oxidase (Phox) (Lambeth, 2004; Wilkinson and Landreth, 2006). The present results indicate that TNF-α and IFN-γ also have cooperative effects on the induction of the catalytic subunit of the NADPH oxidase, the gp91^{phox} (Fig. 2A). As the transcriptional regulation of this subunit is mediated via NF-κB (Gauss et al., 2007), the cooperative effects between the two cytokines tested on gp91^{phox} expression are probably related to their cooperative induction of NF-κB activation. However, the fact that IFN-γ induced NF-κB activation similarly to TNF-α but failed to induce the expression of gp91^{phox} (Fig. 2A, C), strongly suggests that TNF-α activates additional transcription factors also needed for the efficient expression of gp91^{phox} (and similarly for COX-2).

As NO rapidly reacts with the superoxide anion to form the potent oxidant peroxynitrite, our results suggested that the coexposure to TNF-α and IFN-γ could result in increased peroxynitrite generation, as compared both to control explants or explants exposed to each cytokine alone. Peroxynitrite has been proposed to mediate the toxic activities of NO by inducing lipid oxidation and both protein oxidation and nitration (Dawson and Dawson, 1998). To confirm this point, oxidative damage of proteins, as well as protein nitrotyrosination, was assessed. As expected, the combined exposure of explants to TNF-α and IFN-γ resulted both in increased protein carbonyl content (Fig. 3A) and in increased percentage of nitrotyrosine positive motoneurons (Fig. 3B, C), as compared to control explants or explants exposed to each cytokine alone. These results are in agreement with those obtained in the spinal cords of the transgenic mouse model and in ALS patients were it has been described increased protein oxidative damage (Ilieva et al., 2007; Liu et al., 2007), and increased 3-nitrotyrosine immunoreactivity in degenerating spinal cord neurons (Beal et al., 1997; Cha et al., 2000). IFN-γ, when added alone, induced more protein oxidation and nitration than TNF-α alone (Fig. 3A, B). As reactive oxygen species are produced as a consequence of normal aerobic metabolism, it is likely that the increased NO production observed in explants exposed to IFN-γ alone (Fig. 2B) also resulted in increased peroxynitrite production and, consequently, in increased protein oxidation and nitration (see also Bentz et al., 2000). In addition, the effects of TNF-α alone in terms of protein oxidation and nitration (Fig. 3A, B) can be explained by the increased superoxide production as a result of the activity of the gp91^{phox} and COX-2 enzymes induced by this cytokine, as compared to control explants (Fig. 2A). The superoxide produced by these enzymes is expected to react with basal NO to produce peroxynitrite. It is assumed that gp91^{phox} is expressed exclusively by activated microglia in the nervous system (Wilkinson and Landreth, 2006) and in fact, after coexposure to TNF-α and IFN-γ, its immunoreactivity colocalized with that of tomato lectin in our explants (data not shown); by contrast, microglia appear to predominantly express the COX-1 isoform, whereas COX-2 isoform is induced by TNF-α mainly in neurons and astrocytes (Consilvio et al., 2004 and other references therein).

The coexposure to TNF-α and IFN-γ resulted in cooperative effects on apoptotic motoneuron death, measured as the percentage of annexin V positive motoneurons (Fig. 4A). Interestingly, this effect could be abolished by inhibiting the enzymes iNOS with AMT or the NADPH oxidase with apocynin (Fig. 4A). Recently, it has been demonstrated that inhibition of NADPH oxidase with apocynin blocks LPS-mediated motoneuron injury (Li et al., 2008). Moreover, deletion of *Nox* gene significantly slowed disease progression and improved survival in the SOD1 transgenic mice (Marden et al., 2007). Together, these findings reinforce our hypothesis indicating that peroxynitrite and other nitrogen and oxygen reactive species, produced as a result of the activity of the above microglial enzymes, are key factors in neuroinflammation-induced motoneuron death. The coexposure to TNF-α and IFN-γ also resulted in similar increases in the percentage of active caspase-3 positive motoneurons (Fig. 4C, D). These findings are in agreement with those obtained in the transgenic mouse model of ALS, indicating that caspase-3 activation appears before (Wengenack et al., 2004), and at the onset of motor axon loss and that, *in vitro*, caspase-3 activity can be induced by oxidative stress (Pasinelli et al., 2000). In addition, a study in a motoneuron cell line showed that cells transfected with mutant human SOD1 have more annexin V binding than do wild-type cells and cells transfected with the normal human SOD1 (Cookson et al., 2002). In the spinal cord of ALS patients increased caspase-3 activity has also been described, as well as motoneurons with morphological features resembling apoptosis (Martin, 1999; Sathasivam and Shaw, 2005). The

present results also demonstrate that the cytokines TNF-α and IFN-γ, alone or in combination, do not affect the viability of motoneurons in the absence of glial cells (Fig. 5A, B). These findings are in agreement with those in which exposure of purified rat spinal cord embryonic motoneurons to TNF-α (100 ng/ml) did not affect motoneuron survival; however, a redistribution of mitochondria was detected (Stommel et al., 2007). Also in this sense, the combined exposure of a mouse motoneuronal cell line to TNF-α and IFN-γ altered the ultrastructural features and the functionality of mitochondria (Ferri et al., 2008). Mitochondrial failure induced by these cytokines may not be sufficient to induce a death phenotype on purified motoneurons, but may increase their susceptibility to glial-induced oxidative stress, thus causing the release of apoptogenic mitochondrial mediators (Emerit et al., 2004). In addition, TNF-α gene knockout did not affect life span or the extent of motoneuron loss in the SOD1 transgenic mice, thus suggesting that TNF-α alone is not a key factor in motoneuron degeneration (Gowing et al., 2006). These findings can be explained first, because TNF-α has both neuroprotective and neurotoxic effects related to the different signaling pathways activated by their receptors TNFR1 and TNFR2 (Ghezzi and Mennini, 2001) and, consequently, TNF-α acts synergistically/cooperatively with other cytokines (i.e. IFN-γ, present results) to promote neuronal death (see also He et al., 2002); and second, because some proinflammatory cytokines (i.e. IL-1β and TNF-α) have redundant functions *in vivo*; thus, in the knockout of TNF-α an increase in the transcripts encoding for IL-1β was detected (Gowing et al., 2006).

CONCLUSION

In summary, we have developed a new culture system to study the functionality of spinal cord motoneurons in which the activation of microglia with the proinflammatory cytokines TNF-α and IFN-γ reproduces some of the features of ALS in terms of pro-oxidative enzymes expression, protein oxidation and nitration, and apoptotic motoneuron death. Activation of microglial iNOS and NADPH oxidase has been reported to act synergistically to kill neurons (Mander and Brown, 2005); these findings prompt us to propose that the proinflammatory cytokines TNF-α and IFN-γ have complementary roles in inflammation-induced motoneuron death; i.e IFN-γ induces iNOS expression but not gp91^{phox} expression and the opposite occurs in the presence of TNF-α; when the two cytokines act together both enzymes are simultaneously and increasingly induced, thus resulting in increased motoneuron death.

Acknowledgments—This study was supported by the Spanish Ministry of Health through the "Instituto de Salud, Carlos III" grants PI041507, PI051445, PI060680; "Govern Balear, Conselleria d'Economia, Hisenda i Innovació" PROGECIB-3A; "Fundació La Marató de TV3" and "Grups de recerca consolidats" from "Generalitat de Catalunya" (2005SGR00628). M.M. was supported by a pre-doctoral fellowship from the "Fondo de Investigación Sanitaria"; L.T. by a pre-doctoral fellowship from "Govern Balear, Conselleria d'Economia, Hisenda i Innovació" and M.G.-F. by a pre-doctoral fellowship from the "Universitat de Lleida."

REFERENCES

Almer G, Vukosavic S, Romero N, Przedborski S (1999) Inducible nitric oxide synthase up-regulation in a transgenic mouse model of familial amyotrophic lateral sclerosis. J Neurochem 72:2415–2425.

Arce V, Garces A, de Bovis B, Filippi P, Henderson C, Pettmann B deLapeyriere O (1999) Cardiotrophin-1 requires LIFRbeta to promote survival of mouse motoneurons purified by a novel technique. J Neurosci Res 55:119–126.

Babu GN, Kumar A, Chandra R, Puri SK, Kalita J, Misra UK (2008) Elevated inflammatory markers in a group of amyotrophic lateral sclerosis patients from northern India. Neurochem Res 33:1145–1149.

Banerjee R, Mosley RL, Reynolds AD, Dhar A, Jackson-Lewis V, Gordon PH, Przedborski S, Gendelman HE (2008) Adaptive immune neuroprotection in G93A-SOD1 amyotrophic lateral sclerosis mice. PLoS ONE 3:e2740.

Bao F, Liu D (2003) Peroxynitrite generated in the rat spinal cord induces apoptotic cell death and activates caspase-3. Neuroscience 116:59–70.

Bar-Peled O, Knudson M, Korsmeyer SJ, Rothstein JD (1999) Motor neuron degeneration is attenuated in bax-deficient neurons in vitro. J Neurosci Res 55:542–556.

Beal MF, Ferrante RJ, Browne SE, Matthews RT, Kowall NW, Brown RH Jr (1997) Increased 3-nitrotyrosine in both sporadic and familial amyotrophic lateral sclerosis. Ann Neurol 42:644–654.

Bentz BG, Simmons RL, Haines GK 3rd, Radosevich JA (2000) The yin and yang of nitric oxide: reflections on the physiology and pathophysiology of NO. Head Neck 22:71–83.

Boillee S, Vande Velde C, Cleveland DW (2006) ALS: a disease of motor neurons and their nonneuronal neighbors. Neuron 52: 39–59.

Cha CI, Chung YH, Shin CM, Shin DH, Kim YS, Gurney ME, Lee KW (2000) Immunocytochemical study on the distribution of nitrotyrosine in the brain of the transgenic mice expressing a human Cu/Zn SOD mutation. Brain Res 853:156–161.

Consilvio C, Vincent AM, Feldman EL (2004) Neuroinflammation, COX-2, and ALS—a dual role? Exp Neurol 187:1–10.

Cookson MR, Menzies FM, Manning P, Eggett CJ, Figlewicz DA, McNeil CJ, Shaw PJ (2002) Cu/Zn superoxide dismutase (SOD1) mutations associated with familial amyotrophic lateral sclerosis (ALS) affect cellular free radical release in the presence of oxidative stress. Amyotroph Lateral Scler Other Motor Neuron Disord 3:75–85.

Dawson VL, Dawson TM (1998) Nitric oxide in neurodegeneration. Prog Brain Res 118:215–229.

De Paola M, Diana V, Bigini P, Mennini T (2008) Morphological features and responses to AMPA receptor-mediated excitotoxicity of mouse motor neurons: comparison in purified, mixed anterior horn or motor neuron/glia cocultures. J Neurosci Methods 170:85–95.

Elliott JL (2001) Cytokine upregulation in a murine model of familial amyotrophic lateral sclerosis. Brain Res Mol Brain Res 95:172–178.

Emerit J, Edeas M, Bricaire F (2004) Neurodegenerative diseases and oxidative stress. Biomed Pharmacother 58:39–46.

Ferri A, Nencini M, Cozzolino M, Carrara P, Moreno S, Carri MT (2008) Inflammatory cytokines increase mitochondrial damage in motoneuronal cells expressing mutant SOD1. Neurobiol Dis 32: 454–460.

Francisco-Morcillo J, Hidalgo-Sanchez M, Martin-Partido G (2006) Spatial and temporal patterns of proliferation and differentiation in the developing turtle eye. Brain Res 1103:32–48.

Gauss KA, Nelson-Overton LK, Siemsen DW, Gao Y, DeLeo FR, Quinn MT (2007) Role of NF-kappaB in transcriptional regulation of

the phagocyte NADPH oxidase by tumor necrosis factor-alpha. J Leukoc Biol 82:729–741.

Ghezzi P, Mennini T (2001) Tumor necrosis factor and motoneuronal degeneration: an open problem. Neuroimmunomodulation 9:178–182.

Gibbons HM, Dragunow M (2006) Microglia induce neural cell death via a proximity-dependent mechanism involving nitric oxide. Brain Res 1084:1–15.

Gowing G, Dequen F, Soucy G, Julien JP (2006) Absence of tumor necrosis factor-alpha does not affect motor neuron disease caused by superoxide dismutase 1 mutations. J Neurosci 26:11397–11402.

Graves MC, Fiala M, Dinglasan LA, Liu NQ, Sayre J, Chiappelli F, van Kooten C, Vinters HV (2004) Inflammation in amyotrophic lateral sclerosis spinal cord and brain is mediated by activated macrophages, mast cells and T cells. Amyotroph Lateral Scler Other Motor Neuron Disord 5:213–219.

Green LC, Wagner DA, Glogowski J, Skipper PL, Wishnok JS, Tannenbaum SR (1982) Analysis of nitrate, nitrite, and [^{15}N]nitrate in biological fluids. Anal Biochem 126:131–138.

Hall ED, Oostveen JA, Gurney ME (1998) Relationship of microglial and astrocytic activation to disease onset and progression in a transgenic model of familial ALS. Glia 23:249–256.

Hanisch UK (2002) Microglia as a source and target of cytokines. Glia 40:140–155.

Hartig W, Stieler J, Boerema AS, Wolf J, Schmidt U, Weissfuss J, Bullmann T, Strijkstra AM, Arendt T (2007) Hibernation model of tau phosphorylation in hamsters: selective vulnerability of cholinergic basal forebrain neurons—implications for Alzheimer's disease. Eur J Neurosci 25:69–80.

He BP, Wen W, Strong MJ (2002) Activated microglia (BV-2) facilitation of TNF-alpha-mediated motor neuron death in vitro. J Neuroimmunol 128:31–38.

Henkel JS, Beers DR, Siklos L, Appel SH (2006) The chemokine MCP-1 and the dendritic and myeloid cells it attracts are increased in the mSOD1 mouse model of ALS. Mol Cell Neurosci 31:427–437.

Henkel JS, Engelhardt JI, Siklos L, Simpson EP, Kim SH, Pan T, Goodman JC, Siddique T, Beers DR, Appel SH (2004) Presence of dendritic cells, MCP-1, and activated microglia/macrophages in amyotrophic lateral sclerosis spinal cord tissue. Ann Neurol 55: 221–235.

Hensley K, Fedynyshyn J, Ferrell S, Floyd RA, Gordon B, Grammas P, Hamdheydari L, Mhatre M, Mou S, Pye QN, Stewart C, West M, West S, Williamson KS (2003) Message and protein-level elevation of tumor necrosis factor alpha (TNF alpha) and TNF alpha-modulating cytokines in spinal cords of the G93A-SOD1 mouse model for amyotrophic lateral sclerosis. Neurobiol Dis 14:74–80.

Holmoy T (2008) T cells in amyotrophic lateral sclerosis. Eur J Neurol 15:360–366.

Ilieva EV, Ayala V, Jove M, Dalfo E, Cacabelos D, Povedano M, Bellmunt MJ, Ferrer I, Pamplona R, Portero-Otin M (2007) Oxidative and endoplasmic reticulum stress interplay in sporadic amyotrophic lateral sclerosis. Brain 130:3111–3123.

Kawamata T, Akiyama H, Yamada T, McGeer PL (1992) Immunologic reactions in amyotrophic lateral sclerosis brain and spinal cord tissue. Am J Pathol 140:691–707.

Koopman G, Reutelingsperger CP, Kuijten GA, Keehnen RM, Pals ST, van Oers MH (1994) Annexin V for flow cytometric detection of phosphatidylserine expression on B cells undergoing apoptosis. Blood 84:1415–1420.

Kuno R, Wang J, Kawanokuchi J, Takeuchi H, Mizuno T, Suzumura A (2005) Autocrine activation of microglia by tumor necrosis factor-alpha. J Neuroimmunol 162:89–96.

Lambeth JD (2004) NOX enzymes and the biology of reactive oxygen. Nat Rev Immunol 4:181–189.

Levine RL, Williams JA, Stadtman ER, Shacter E (1994) Carbonyl assays for determination of oxidatively modified proteins. Methods Enzymol 233:346–357.

Li B, Guo YS, Sun MM, Dong H, Wu SY, Wu DX, Li CY (2008) The NADPH oxidase is involved in lipopolysaccharide-mediated motor neuron injury. Brain Res 1226:199–208.

Liu D, Bao F, Wen J, Liu J (2007) Mutation of superoxide dismutase elevates reactive species: comparison of nitration and oxidation of proteins in different brain regions of transgenic mice with amyotrophic lateral sclerosis. Neuroscience 146:255–264.

Mander P, Brown GC (2005) Activation of microglial NADPH oxidase is synergistic with glial iNOS expression in inducing neuronal death: a dual-key mechanism of inflammatory neurodegeneration. J Neuroinflammation 2:20.

Marden JJ, Harraz MM, Williams AJ, Nelson K, Luo M, Paulson H, Engelhardt JF (2007) Redox modifier genes in amyotrophic lateral sclerosis in mice. J Clin Invest 117:2913–2919.

Martin LJ (1999) Neuronal death in amyotrophic lateral sclerosis is apoptosis: possible contribution of a programmed cell death mechanism. J Neuropathol Exp Neurol 58:459–471.

McGeer PL, McGeer EG (2002) Inflammatory processes in amyotrophic lateral sclerosis. Muscle Nerve 26:459–470.

Mhatre M, Floyd RA, Hensley K (2004) Oxidative stress and neuroinflammation in Alzheimer's disease and amyotrophic lateral sclerosis: common links and potential therapeutic targets. J Alzheimers Dis 6:147–157.

Mir M, Tolosa L, Asensio VJ, Llado J, Olmos G (2008) Complementary roles of tumor necrosis factor alpha and interferon gamma in inducible microglial nitric oxide generation. J Neuroimmunol 204:101–109.

Nakao S, Ogtata Y, Shimizu E, Yamazaki M, Furuyama S, Sugiya H (2002) Tumor necrosis factor alpha (TNF-alpha)-induced prostaglandin E_2 release is mediated by the activation of cyclooxygenase-2 (COX-2) transcription via NFkappaB in human gingival fibroblasts. Mol Cell Biochem 238:11–18.

Pasinelli P, Houseweart MK, Brown RH Jr, Cleveland DW (2000) Caspase-1 and -3 are sequentially activated in motor neuron death in Cu,Zn superoxide dismutase-mediated familial amyotrophic lateral sclerosis. Proc Natl Acad Sci U S A 97:13901–13906.

Peluffo H, Shacka JJ, Ricart K, Bisig CG, Martinez-Palma L, Pritsch O, Kamaid A, Eiserich JP, Crow JP, Barbeito L, Estevez AG (2004) Induction of motor neuron apoptosis by free 3-nitro-L-tyrosine. J Neurochem 89:602–612.

Poloni M, Facchetti D, Mai R, Micheli A, Agnoletti L, Francolini G, Mora G, Camana C, Mazzini L, Bachetti T (2000) Circulating levels of tumour necrosis factor-alpha and its soluble receptors are increased in the blood of patients with amyotrophic lateral sclerosis. Neurosci Lett 287:211–214.

Rothstein JD, Jin L, Dykes-Hoberg M, Kuncl RW (1993) Chronic inhibition of glutamate uptake produces a model of slow neurotoxicity. Proc Natl Acad Sci U S A 90:6591–6595.

Sargsyan SA, Monk PN, Shaw PJ (2005) Microglia as potential contributors to motor neuron injury in amyotrophic lateral sclerosis. Glia 51:241–253.

Sasaki S, Shibata N, Komori T, Iwata M (2000) iNOS and nitrotyrosine immunoreactivity in amyotrophic lateral sclerosis. Neurosci Lett 291:44–48.

Sathasivam S, Shaw PJ (2005) Apoptosis in amyotrophic lateral sclerosis—what is the evidence? Lancet Neurol 4:500–509.

Sedel F, Bechade C, Vyas S, Triller A (2004) Macrophage-derived tumor necrosis factor alpha, an early developmental signal for motoneuron death. J Neurosci 24:2236–2246.

Shaw PJ (2005) Molecular and cellular pathways of neurodegeneration in motor neurone disease. J Neurol Neurosurg Psychiatry 76:1046–1057.

Soler RM, Egea J, Mintenig GM, Sanz-Rodriguez C, Iglesias M, Comella JX (1998) Calmodulin is involved in membrane depolarization-mediated survival of motoneurons by phosphatidylinositol-3 kinase- and MAPK-independent pathways. J Neurosci 18:1230–1239.

Stommel EW, van Hoff RM, Graber DJ, Bercury KK, Langford GM, Harris BT (2007) Tumor necrosis factor-alpha induces changes in mitochondrial cellular distribution in motor neurons. Neuroscience 146:1013–1019.

Tolosa L, Mir M, Asensio VJ, Olmos G, Llado J (2008) Vascular endothelial growth factor protects spinal cord motoneurons against glutamate-induced excitotoxicity via phosphatidylinositol 3-kinase. J Neurochem 105:1080–1090.

Troost D, van den Oord JJ, de Jong JM, Swaab DF (1989) Lymphocytic infiltration in the spinal cord of patients with amyotrophic lateral sclerosis. Clin Neuropathol 8:289–294.

Tsuchida T, Ensini M, Morton SB, Baldassare M, Edlund T, Jessell TM, Pfaff SL (1994) Topographic organization of embryonic motor neurons defined by expression of LIM homeobox genes. Cell 79:957–970.

Turner MR, Cagnin A, Turkheimer FE, Miller CC, Shaw CE, Brooks DJ, Leigh PN, Banati RB (2004) Evidence of widespread cerebral microglial activation in amyotrophic lateral sclerosis: an [^{11}C] (R)-PK11195 positron emission tomography study. Neurobiol Dis 15: 601–609.

Vermeren M, Maro GS, Bron R, McGonnell IM, Charnay P, Topilko P, Cohen J (2003) Integrity of developing spinal motor columns is regulated by neural crest derivatives at motor exit points. Neuron 37:403–415.

Wen W, Sanelli T, Ge W, Strong W, Strong MJ (2006) Activated microglial supernatant induced motor neuron cytotoxicity is associated with upregulation of the TNFR1 receptor. Neurosci Res 55:87–95.

Wengenack TM, Holasek SS, Montano CM, Gregor D, Curran GL, Poduslo JF (2004) Activation of programmed cell death markers in ventral horn motor neurons during early presymptomatic stages of amyotrophic lateral sclerosis in a transgenic mouse model. Brain Res 1027:73–86.

Wetts R, Vaughn JE (2001) Development of cholinergic terminals around rat spinal motor neurons and their potential relationship to developmental cell death. J Comp Neurol 435:171–183.

Weydt P, Moller T (2005) Neuroinflammation in the pathogenesis of amyotrophic lateral sclerosis. Neuroreport 16:527–531.

Wilkinson BL, Landreth GE (2006) The microglial NADPH oxidase complex as a source of oxidative stress in Alzheimer's disease. J Neuroinflammation 3:30.

Yamada T, Pfaff SL, Edlund T, Jessell TM (1993) Control of cell pattern in the neural tube: motor neuron induction by diffusible factors from notochord and floor plate. Cell 73:673–686.

Zhang R, Gascon R, Miller RG, Gelinas DF, Mass J, Hadlock K, Jin X, Reis J, Narvaez A, McGrath MS (2005) Evidence for systemic immune system alterations in sporadic amyotrophic lateral sclerosis (sALS). J Neuroimmunol 159:215–224.

Zhao W, Xie W, Le W, Beers DR, He Y, Henkel JS, Simpson EP, Yen AA, Xiao Q, Appel SH (2004) Activated microglia initiate motor neuron injury by a nitric oxide and glutamate-mediated mechanism. J Neuropathol Exp Neurol 63:964–977.

(Accepted 21 May 2009)
(Available online 27 May 2009)